Br-Assisted Ostwald Ripening of Au Nanoparticles under H2O2 Redox

ARTICLE *in* CRYSTAL GROWTH & DESIGN · NOVEMBER 2011

Impact Factor: 4.89 · DOI: 10.1021/cg201243n

8 AUTHORS, INCLUDING:

Jihye Choi
Stanford University
34 PUBLICATIONS **477** CITATIONS
SEE PROFILE

Joseph Park
University of North Carolina at Charlotte
26 PUBLICATIONS **462** CITATIONS
SEE PROFILE

Jin-suck Suh
Yonsei University
295 PUBLICATIONS **7,009** CITATIONS
SEE PROFILE

Seungjoo Haam
Yonsei University
201 PUBLICATIONS **3,763** CITATIONS
SEE PROFILE

CRYSTAL GROWTH & DESIGN

Communication

pubs.acs.org/crystal

Br-Assisted Ostwald Ripening of Au Nanoparticles under H_2O_2 Redox

Eunji Jang,[†] Eun-Kyung Lim,[†] Jihye Choi,[†] Joseph Park,[†] Yong-Jung Huh,[‡] Jin-Suck Suh,[§,∥,⊥] Yong-Min Huh,*[,§,∥,⊥] and Seungjoo Haam*[,†]

[†]Department of Chemical and Biomolecular Engineering, Yonsei University, Seoul 120-749, South Korea

[‡]School of Mechatronics Engineering, Korea University of Technology and Education, Chungnam 330-708, South Korea

[§]Department of Radiology, Yonsei University, Seoul 120-752, South Korea

[∥]YUHS-KRIBB Medical Convergence Research Institute, Seoul 120-752, South Korea

[⊥]Severance Biomedical Science Institute (SBSI), Seoul 120-752, South Korea

Supporting Information

ABSTRACT: In nanomaterials synthesis, Ostwald ripening is a postsynthetic problem that is one obstacle for common utilization of nanomaterials. Herein, we report an unprecedented Ostwald ripening mechanism resulting from the simple combination of hydrogen peroxide (H_2O_2) and cetyltrimethylammonium bromide (CTAB)-stabilized gold nanoparticles (AuNPs) at room temperature. In this ripening process, H_2O_2 redox induces simultaneous dissolution and growth of AuNPs where bromide (Br^-) from CTAB helps to form $AuBr_2^-$ in aqueous solution at room temperature. This understanding will provide basic strategies for advanced designs and development of various nanomaterials.

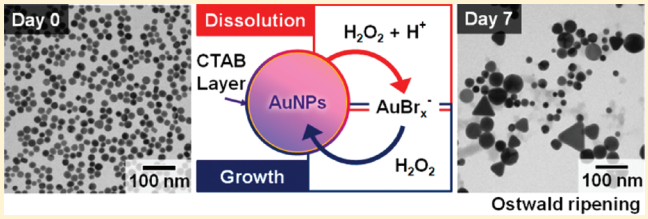

Nanosized particles have been employed in many applications due to their distinct physicochemical properties. However, nanosized particles are problematic in that their nanoscale surface curvature is intrinsically metastable, leading to postsynthetic problems such as aggregation or coarsening, which can lead to flaws in the necessary nanoparticle traits. Ostwald ripening, one of these postsynthetic problems, is a phenomenon related to the growth of larger particles at the expense of smaller ones. This results in increased average size, particle size distribution broadening, and number density decrease.[1] Ostwald ripening during metal nanoparticle synthesis is mainly induced by high temperature, where high thermal energy mobilizes the activated surface atoms of nanoparticles.[1a−d] In this study, we identified an atypical Ostwald ripening at room temperature in cetyltrimethylammonium bromide (CTAB)-stabilized gold nanoparticles (AuNPs) caused by hydrogen peroxide (H_2O_2)-redox. In this ripening process, H_2O_2 and bromide (Br^-) induce oxidation and reduction of AuNPs simultaneously.

CTAB-stabilized 18.0 ± 3.1 nm AuNPs were prepared by the seed-mediated method (Figure 1a).[2] After elimination of the impurities (e.g., ascorbic acid) by centrifugation, AuNPs were mixed with a 35 wt % H_2O_2 solution (0.1 volume fraction) at room temperature ([Au] = 0.2 mM, [CTAB] = 9.5 mM, [HCl] = 0.3 mM). HCl solution was used to control the proton (H^+) concentration in the solution. All the reactions were performed in dark condition to avoid Au reduction by light.[3]

In transmission electron microscopy (TEM) images, CTAB-stabilized AuNPs exhibited some morphological changes after exposure to H_2O_2 (Figure 1 and Figure S1 in the Supporting Information). We observed a broadening in particle size distribution (PSD) that began at day 1, followed by overall growth of AuNPs with random shapes from day 3 (Figure S1). The growth of AuNPs continued even after precipitation began at day 7 (Figure S2). We statistically analyzed changes in PSD using TEM images, and we confirmed that PSD had a Gaussian distribution and log−normal distribution on days 0−3 and on

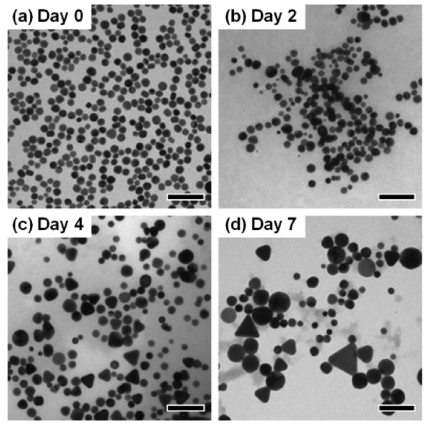

Figure 1. Representative TEM images for CTAB-stabilized AuNPs exposed to H_2O_2 at (a) day 0, (b) day 2, (c) day 4, and (d) day 7. The average sizes of AuNPs are (a) 18.0 ± 3.1 nm, (b) 15.9 ± 6.2 nm, (c) 22.4 ± 8.6 nm, and (d) 29.8 ± 12.7 nm, respectively. All scale bars are 100 nm.

Received: September 21, 2011
Revised: November 20, 2011
Published: November 28, 2011

days 4–7, respectively (Figure S1 (b)). This is consistent with previous Ostwald ripening studies,[1a] but it should be noted that the average particle size temporarily decreased before overall growth was observed; 18.0 ± 3.1 nm at day 0, 15.9 ± 6.2 nm at day 2, 22.4 ± 8.6 nm at day 4, and 29.8 ± 12.7 nm at day 7. This tendency observed from TEM analysis was also consistent with the changes in UV–vis spectra of AuNPs exposed to H_2O_2; the absorbance intensity dramatically decreased on days 1–2, followed by a red-shift in the absorbance peak (ca. 10 nm) and broadening of the full-width-half-maximum after day 3 (Figure S3).

H_2O_2 can oxidize CTAB-stabilized Au nanostructures to $AuBr_4^-$, the absorbance peak of which appears at approximately 400 nm under acidic conditions.[4] We confirmed that CTAB-stabilized AuNPs exposed to H_2O_2 were completely oxidized to $AuBr_4^-$ as H^+ ions were provided up to 3.0 mM (Figure S4(a)). Conversely, under rather mild conditions, the absorbance intensity in the UV–vis spectra slowly decreased without any partial changes around 400 nm in the spectra, indicating that mild oxidation induced the formation of colorless $AuBr_2^-$.[3] We measured the $AuBr_2^-$ concentration in the transparent supernatant of the ripening solution by inductively coupled plasma–atomic emission spectroscopy (ICP-AES), confirming that $AuBr_2^-$ formation was proportional to the H^+ concentration in solution (Figure S4(b)).

In the presence of $AuBr_2^-$ with AuNPs and H_2O_2, we hypothesized an electrochemical mechanism of Ostwald ripening at room temperature in CTAB-stabilized AuNPs; H_2O_2 redox induced the simultaneous oxidation of the AuNPs and reduction of $AuBr_2^-$, which resulted in growth of larger particles at the expense of smaller ones without conventional thermal energy (Figure 2). H_2O_2 has two electrochemical

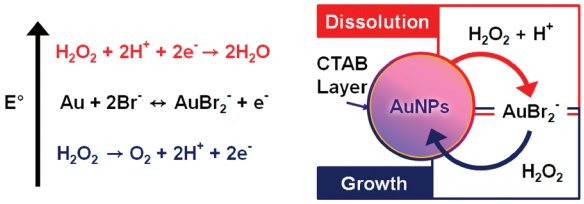

Figure 2. Diagram illustrating the Ostwald ripening of CTAB-stabilized AuNPs by H_2O_2 redox; simultaneous reduction and oxidation between AuNPs and $AuBr_2^-$ induced by H_2O_2 redox.

potentials. One is the reduction potential for H_2O_2/H_2O (1.7 V), and the other is the oxidation potential for H_2O_2/O_2 (0.695 V).[5] Because the reduction potential for $AuBr_2^-/Au$ (0.96 V)[5] lies between the two potentials of H_2O_2, the exposure of AuNPs to H_2O_2 can cause both the oxidation of AuNPs (eq 1) and the reduction of $AuBr_2^-$ (eq 2).

$$\text{Oxidation: } H_2O_2 + 2H^+ + 2Au + 4Br^- = 2AuBr_2^- + 2H_2O \quad (1)$$

$$\text{Reduction: } H_2O_2 + 2AuBr_2^- = 2Au + 2H^+ + 4Br^- + O_2 \quad (2)$$

As previously mentioned, H^+ accelerated the dissolution of AuNPs to $AuBr_2^-$ (eq 1). Likewise, Br^- also favored the dissolution of AuNPs in the ripening solution. In contrast, the lack of CTAB in the ripening solution resulted in aggregation of AuNPs without any morphological changes (Figure S5 of the Supporting Information). Therefore, two candidate mechanisms may be possible: (i) H_2O_2 could oxidize AuNPs after aggregation with sufficient H^+ and Br^- concentration in the ripening solution and (ii) Br^- may not be replaced with chloride (Cl^-) in the oxidation of AuNPs even though excess Cl^- exists in the ripening solution. To verify these mechanisms, we used citrate-stabilized AuNPs prepared by the Turkevich method to exclude Br^- from CTAB. We controlled the halide concentration using HBr and HCl (Figure 3). The results

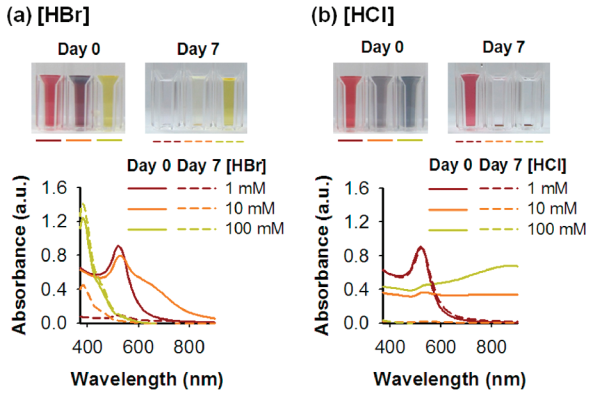

Figure 3. UV–vis absorbance spectra and digital pictures of citrate-stabilized AuNPs (a) dissolved in HBr solution and (b) aggregated in HCl solution after exposure to H_2O_2.

showed that the oxidation of AuNPs occurred after aggregation ([HBr] = 10 mM, Figure 3a), while no oxidation was observed on AuNPs exposed to H_2O_2 with Cl^- regardless of aggregation (Figure 3b).

This may be due to the formation of Br_3^- by H_2O_2 redox, which plays a catalytic role for AuNPs oxidation.[6] It has been reported that Br_3^- can be formed under coexistence of Br^- and Br_2 in water ($Br_3^- = Br^- + Br_2$, $K_c = 0.063$) in a Au dissolution system with HBr/Br_2.[6a,b] Because H_2O_2 has an oxidation potential able to reduce Br^- to Br_2 (Br^-/Br_2, 1.08 V),[6c] Br_3^- can be formed and act as catalyst for dissolving AuNPs into $AuBr_2^-$ in this CTAB/H_2O_2 system.

Finally, we confirmed whether two distinct reactions (eqs 1 and 2) occur at the same time. If so, the $AuBr_2^-$ concentration would reach equilibrium in the ripening solution. As we monitored the change in $AuBr_2^-$ concentration in the ripening solution under conditions identical to those shown in Figure 1, (i) half of the AuNPs were oxidized to $AuBr_2^-$ (0.104 ± 0.003 mM) at day 1, (ii) the $AuBr_2^-$ concentration seemed to reach a specific concentration (0.136 ± 0.008 mM) at day 7, and then (iii) the concentration remained unchanged even after the AuNPs completely precipitated (0.136 ± 0.004 mM) (Figure 4a). Judging from the TEM images that showed gradual AuNP growth with PSD broadening, the constant $AuBr_2^-$ concentration in the ripening solution proved that oxidation of AuNPs (eq 1) and reduction of $AuBr_2^-$ (eq 2) coincided. This simultaneous oxidation and reduction led to Ostwald ripening, resulting in the dissolution of smaller AuNPs with high curvature followed by reduction of $AuBr_2^-$ on larger AuNPs, leading to growth. We also approximated the total number of AuNPs in the ripening solution by combining the changes in $AuBr_2^-$ concentration with PSD analysis, which showed one feature of Ostwald ripening in that the number density of the AuNPs declined with average size growth (Table S1 of the Supporting Information and Figure 4b).

dx.doi.org/10.1021/cg201243n | Cryst. Growth Des. 2012, 12, 37–39

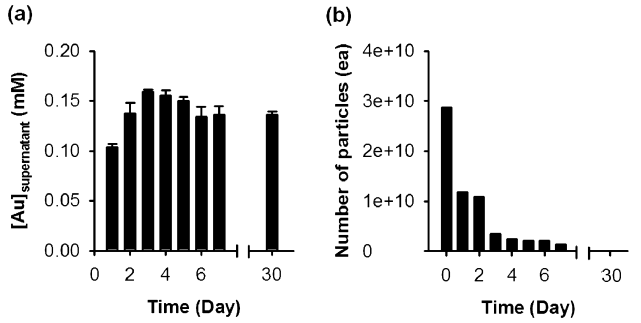

Figure 4. (a) $AuBr_2^-$ concentrations in the daily supernatants of the ripening solution under conditions identical to those described in Figure 1; (b) approximate numbers of AuNPs in the ripening solution with respect to time.

In conclusion, we reported Ostwald ripening of CTAB-stabilized AuNPs originating from the combination of redox between H_2O_2 and AuNPs under weakly acidic conditions. Br^-, in particular, played a crucial role in the oxidation of AuNPs to $AuBr_2^-$, which brought about Ostwald ripening at room temperature. Considering the expansion in applications of metal nanomaterials, this investigation of postsynthetic problems at room temperature is of general importance, especially in the context of electrochemical Ostwald ripening, and it may serve as a foundation for advanced designs and development of nanosized materials.

■ ASSOCIATED CONTENT

Supporting Information

Experimental methods and results of supporting experiments. This material is available free of charge via the Internet at http://pubs.acs.org.

■ AUTHOR INFORMATION

Corresponding Author

*E-mail: haam@yonsei.ac.kr; ymhuh@yuhs.ac.

■ ACKNOWLEDGMENTS

This work was supported by a National Research Foundation grant funded by the Korean government (MEST) (2011-0027724). This study was also supported by a grant under the Korea Health 21 R&D Project funded by the Ministry of Health &Welfare, Republic of Korea (A101954).

■ REFERENCES

(1) (a) Simonsen, S. B.; Chorkendorff, I.; Dahl, S.; Skoglundh, M.; Sehested, J.; Helveg, S. *J. Am. Chem. Soc.* **2010**, *132*, 7968. (b) Yang, F.; Chen, M. S.; Goodman, D. W. *J. Phys. Chem. C* **2009**, *113*, 254. (c) Meli, L.; Freen, P. F. *ACS Nano* **2008**, *2*, 1305. (d) Alloyeau, D.; Prévot, G.; Le Bouar, Y.; Oikawa, T.; Langlois, C.; Loiseau, A.; Ricolleau, C. *Phys. Rev. Lett.* **2010**, *13*, 255901. (e) Di Vece, M.; Grandjean, D.; Van Bael, M. J.; Romero, C. P.; Wang, X.; Decoster, S.; Vantomme, A.; Lievens, P. *Phys. Rev. Lett.* **2008**, *100*, 236105. (f) Redmond, P. L.; Hallock, A. J.; Brus, L. E. *Nano Lett.* **2005**, *5*, 131.

(2) Choi, J.; Yang, J.; Park, J.; Kim, E.; Suh, J. S.; Huh, Y. M.; Haam, S. *Adv. Funct. Mater.* **2011**, *21*, 1082.

(3) (a) Soejima, T.; Kimizuka, N. *J. Am. Chem. Soc.* **2009**, *131*, 14407. (b) Eustis, S.; Hsu, H.; El-Sayed, M. A. *J. Phys. Chem. B* **2005**, *109*, 4811. (c) Eustis, S.; El-Sayed, M. A. *J. Phys. Chem. B* **2006**, *110*, 14014. (d) Jin, R.; Cao, Y.; Mirkin, C. A.; Kelly, K. L.; Schatz, G. C.; Zheng, J. G. *Science* **2001**, *294*, 1901. (e) Xue, C.; Metraux, C. S.; Millstone, J. E.; Mirkin, C. A. *J. Am. Chem. Soc.* **2008**, *130*, 8337.

(4) (a) Ni, W.; Kou, X.; Yang, Z.; Wang, J. *ACS Nano* **2008**, *2*, 677. (b) Tsung, C. K.; Kou, X.; Shi, Q.; Zhang, J.; Yeung, M. H.; Wang, J.; Stucky, G. D. *J. Am. Chem. Soc.* **2006**, *128*, 5352.

(5) Bard, A. J.; Parsons, R.; Jordan, J. *Standard potentials in aqueous solution*, 1st ed.; CRC Press: Boca Raton, FL; New York, 1985.

(6) (a) Pesic, B.; Sergent, R. H. *Metall. Trans. B* **1993**, *24*, 419. (b) Kurniawan, F. Ph.D. Dissertation, Resensburg University, 2008. (c) Bray, W. C.; Livingston, R. S. *J. Am. Chem. Soc.* **1923**, *45*, 1251.

Supporting information

Experimental methods

Materials

Gold(III) chloride trihydrate ($HAuCl_4 \cdot 3H_2O$), cetyltrimethylammonium bromide (CTAB), sodium borohydride, silver nitrate, L-ascorbic acid, trisodium citrate, and 35 wt% hydrogen peroxide (H_2O_2) were obtained from Sigma-Aldrich (St. Louis, MO, USA). Ultrapure deionized water was used for all of the syntheses.

Preparation of CTAB-stabilized Au nanoparticles

CTAB-stabilized gold nanoparticles (AuNPs) were synthesized using the seed-mediated growth method in aqueous CTAB solution.[S1] Briefly, seed solutions were prepared by injecting 0.6 mL of 0.01 M ice-cold sodium borohydride solution into a mixture containing 0.25 mL of 0.01 M $HAuCl_4 \cdot 3H_2O$ solution and 7.5 mL of 0.095 M CTAB solution with vigorous stirring. Then, the seed solution was reacted for 2 min and aged for 3 h. A growth solution was prepared by mixing 10 μL of 0.01 M silver nitrate solution, 0.5 mL of 0.01 M $HAuCl_4 \cdot 3H_2O$ solution and 9.5 mL of 0.095 M CTAB solution with stirring. The addition of 55 μL of 100 mM ascorbic acid solution to the growth solution resulted in a color change from yellow to colorless. AuNP growth was initiated by introducing 20 μL of seed solution into the growth solution. Then, the color of the solution turned reddish over ten minutes. The product solution was left for 12 h at room temperature and then centrifuged at 15,000 rpm for 30 min. The precipitated AuNPs were redispersed in 0.095 M CTAB solution. Every step of the AuNP preparation was performed at room temperature.

Effect of Cl^- existence on the Ostwald ripening of citrate-stabilized AuNPs

Citrate-stabilized AuNPs were prepared by the Turkevich method using citrate instead of CTAB.[S2] One milliliter of 1 wt% $HAuCl_4$ solution and 5 ml of 1 wt% trisodium citrate solution were injected into 100 ml of boiling deionized water. After boiling for 30 minutes, the reddish citrate-stabilized AuNPs were concentrated by centrifugation at 3000 rpm for 10 min using an Amicon (MWCO 50K) centrifuge. Then, the citrate-stabilized AuNPs and H_2O_2 were dispersed in 1, 10, 100 mM HCl and HBr solutions ([Au] = 0.2 mM, H_2O_2 of 0.1 volume fraction). Optical changes in AuNPs caused by exposure to H_2O_2 were observed with the naked eye and by UV-Vis spectroscopy.

Effect of Br^- concentration to Ostwald ripening of CTAB-stabilized AuNPs

After centrifuging twice, solutions of AuNPs dispersed in 19 mM CTAB solution, deionized water, and 9.5 mM NaBr with 9.5 mM CTAB (total $[Br^-]$ = 19 mM) solution were prepared, respectively. These AuNPs were then mixed with H_2O_2 ([Au] = 0.2 mM, [HCl] = 0.3 mM, H_2O_2 of 0.1 volume fraction). Morphological changes in the AuNPs were observed via TEM analysis and spectral changes were observed by UV-Vis spectroscopy.

Measurements

The size and morphology of the AuNPs were observed using transmission electron microscopy (TEM, JEM-1011, JEOL, Japan) at an acceleration voltage of 80 kV. Particle size was measured manually using ImageJ software with more than ten TEM images taken for each sample. In cases of polygonal AuNPs, the diagonal length was measured and used as the particle size. The UV-Vis absorbance spectra of the AuNPs were obtained using an Optizen UV-Vis spectrometer (2120UV; Mecasys, Korea). The full-width-half-maximum (FWHM) was measured as twice the width of the right half in the absorbance spectra. The amounts of $AuBr_2^-$ in the ripening solution were quantified using inductively coupled plasma atomic emission spectrometry (ICP-AES, Thermo Electron Corporation, USA). The absorptions of Br^- and Cl^- on the AuNPs were confirmed using X-ray photoelectron spectroscopy (XPS, ESCALAB 220i-XL, USA).

References

(S1) Choi, J.; Yang, J.; Park, J.; Kim, E.; Suh, J. S.; Huh, Y. M.; Haam, S. *Adv. Funct. Mater.,* **2011**, *21*, 1082-1088.
(S2) Frens, G. *Nat. Phys. Sci*., **1973**, *241*, 20-22.

TEM analysis of Ostwald ripening of CTAB-stabilized AuNPs exposed to H_2O_2

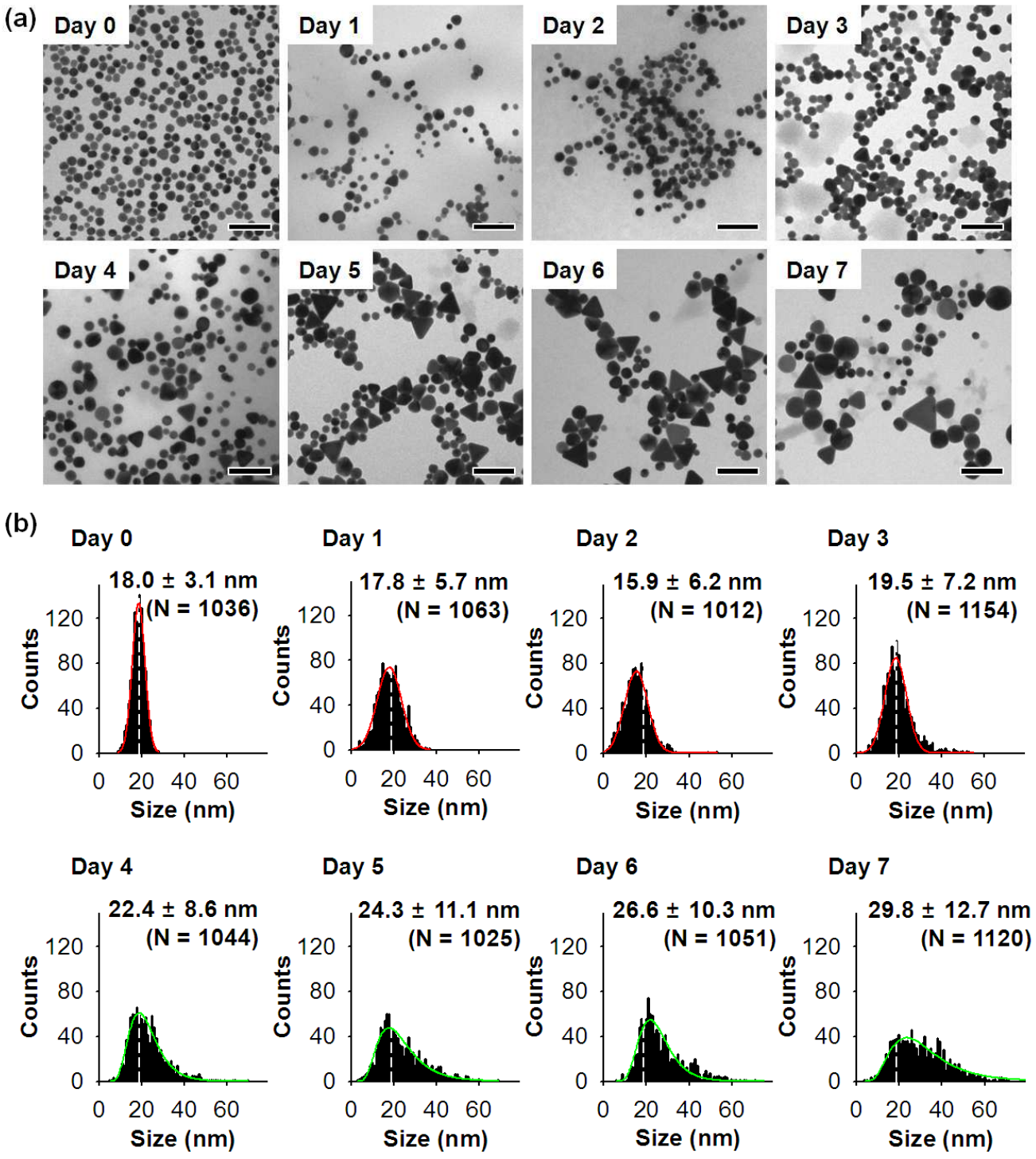

Figure S1. (a) Representative TEM images illustrating the Ostwald ripening of CTAB-stabilized AuNPs exposed to H_2O_2 and (b) their particle size distribution based on TEM images. White dashed lines represent 18.0 nm, red fit lines show the Gaussian distribution and green fit lines correspond to the log-normal distribution. N indicates the number of particles included in each particle size distribution.

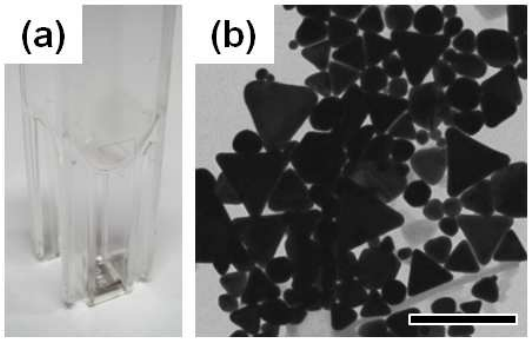

Figure S2. Complete precipitation and transparent supernatant of CTAB-stabilized AuNPs exposed to H_2O_2 over a month. (a) Digital image and (b) TEM image of the precipitates. The scale bar is 300 nm. The average particle size is 73.2 ± 39.7 nm (N = 106).

UV-Vis spectral analysis of Ostwald ripening of CTAB-stabilized AuNPs exposed to H_2O_2

We analyzed the optical property changes of CTAB-stabilized AuNPs exposed to H_2O_2 over time. The color of the AuNP solution became gradually lighter from red-pink (at day 1) to violet-pink (day 7) with time. In the UV-Vis spectra, the absorbance peak was red-shifted (ca. 10 nm) and broadened at day 3 due to the particle growth and the appearance of assorted shapes of AuNPs. A closer inspection of the spectral changes of the AuNPs revealed a fluctuation in the intensity of the absorbance peak and full width at half maximum (FWHM).

(I) Intensity of the absorbance peak
In the early dissolution stage, the reduction in the size and numbers of AuNPs markedly reduced the absorbance intensity. At day 3, however, the intensity increased abruptly, and then decreased again. This fluctuation could be interpreted as the result of interplay between the increase in average size with random shape formation and the decrease in the total number of particles. Although the growth of AuNPs restored the absorbance peak intensity, the continuous reduction in the number of AuNPs neutralized these gains.

(II) Full width at half maximum (FWHM)
FWHM is known to increase as the particle size distribution (PSD) broadens. However, the FWHM in Figure S3 (c) seems to coincide with the appearance of larger AuNPs in PSD (Figure S1 (b)) rather than PSD broadening itself. A decrease in FWHM was also observed with precipitation on day 7.

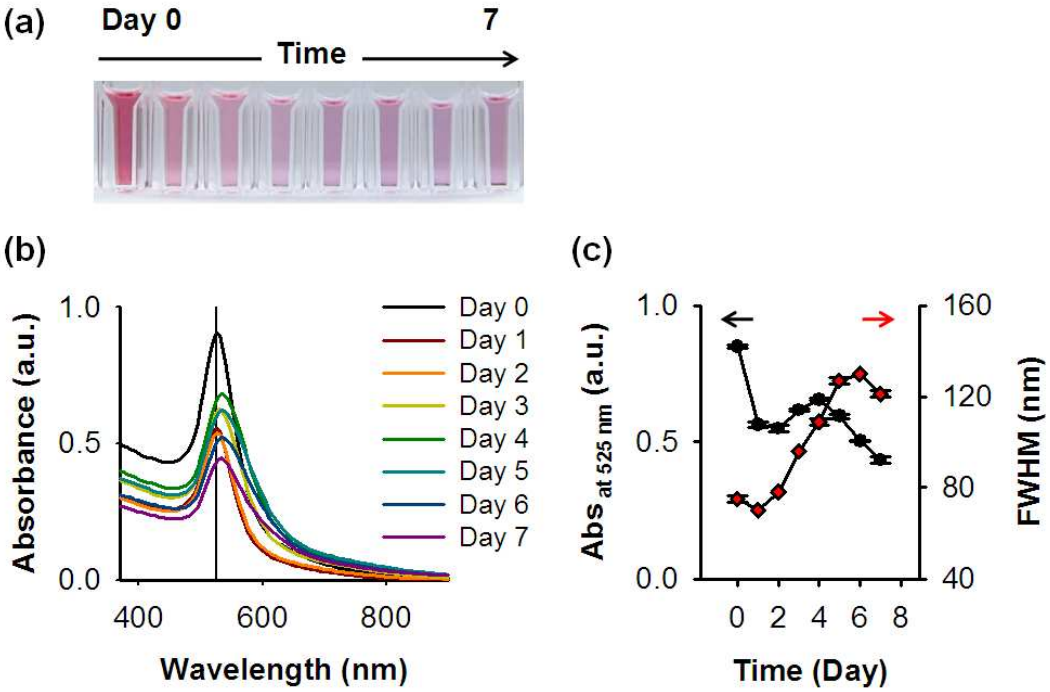

Figure S3. Change in the optical properties of CTAB-stabilized AuNPs exposed to H_2O_2 over time: (a) digital picture, (b) UV-Vis absorbance spectra (black line for 520 nm) and (c) changes in UV-Vis absorbance intensity at 525 nm (black) and FWHM (red).

Dissolution of CTAB-stabilized AuNPs exposed to H_2O_2 in acidic conditions

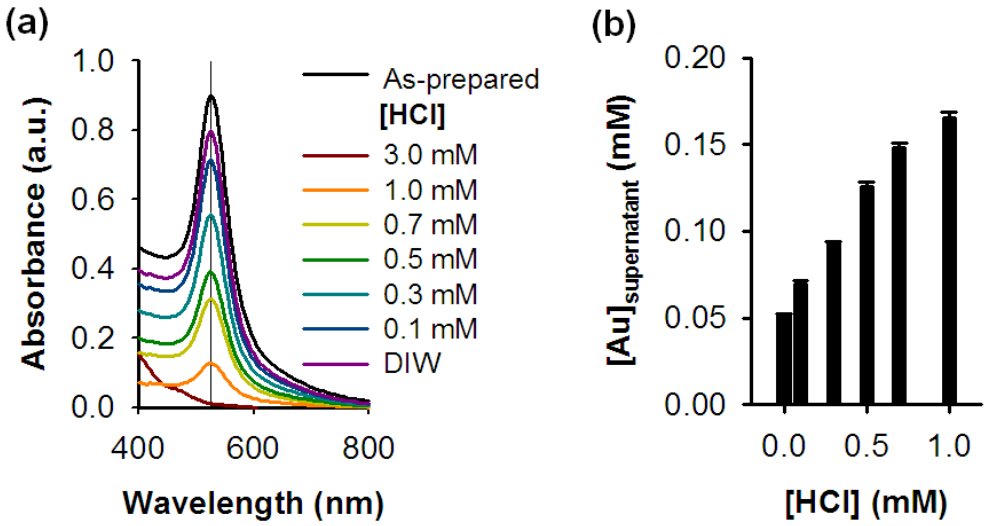

Figure S4. AuNP dissolution due to H_2O_2 redox as a function of H^+ concentration: (a) UV-Vis absorbance spectra of CTAB-stabilized AuNPs exposed to H_2O_2 solution by varying the concentrations of HCl and (b) $AuBr_2^-$ in the supernatants. Both results were measured one day after exposure to H_2O_2.

The effect of bromide in Ostwald ripening of CTAB-stabilized AuNPs exposed to H_2O_2

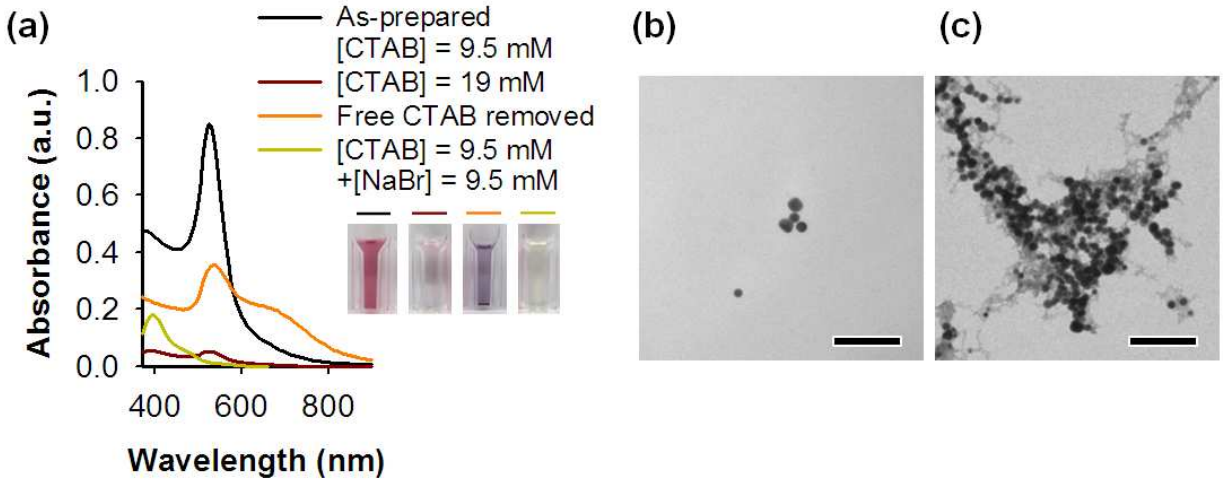

Figure S5. Effect of Br^- concentration on the dissolution of AuNPs by H_2O_2 redox: (a) UV-Vis spectra and digital pictures of CTAB-stabilized AuNPs exposed to H_2O_2. The black line corresponds to as-prepared CTAB-stabilized AuNPs ([CTAB] = 9.5 mM), the red line represents the AuNPs with doubled CTAB concentration ([CTAB] = 19 mM) exposed to H_2O_2 after one day, the orange line denotes the free CTAB-removed AuNPs by centrifugation and redispersion in deionized water followed by exposure to H_2O_2 after seven days, and the yellow line represents AuNPs in [CTAB] = 9.5 mM with [NaBr] = 9.5 mM exposed to H_2O_2 after one day. [Au] = 0.2 mM, [HCl] = 0.3 mM. (b) TEM images for the red line (c) and the orange line in (a). A TEM image for the yellow line was not available. Scale bars are 100 nm.

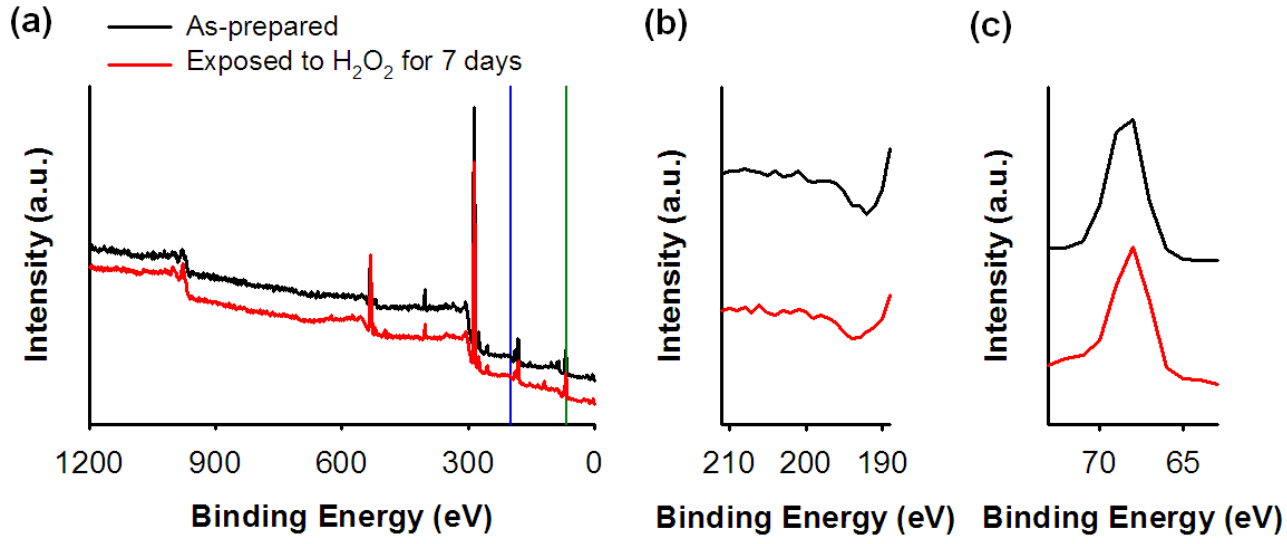

Figure S6. (a) XPS spectra of CTAB-stabilized AuNPs as-prepared and exposed to H_2O_2 for seven days (Au = 0.2 mM, [CTAB] = 9.5 mM, [HCl] = 0.3 mM). The blue line at 199 eV is for Cl 2p and the green line at 67 eV is for Br 3d. XPS spectra of (b) Cl 2p and (c) Br 3d.

Approximate number of AuNPs in the ripening solution

We approximated the total number of AuNPs in solution by combining data for $AuBr_2^-$ concentrations (Figure S5) and statistical analysis (Figure S1 (b)). First, we found the mass of AuNPs in solution from Figure S5 using the atomic weight of Au (79 g/mol). Second, we set the number of AuNPs we counted in Figure S1 (b) to one set. Then, we found the mass of AuNPs per set using the density of Au (19.3 g/cm^{-3}). Third, we determined how many sets were in solution by dividing the mass of the AuNPs in solution by the mass of AuNPs per set. Finally, we found the total number of AuNPs by multiplying the number of sets by the number of AuNPs per set.

Table S1. Approximate number of AuNPs in solution.

Time (Day)	[a] Mass $AuBr_2^-$ (umol)	[b] Mass AuNPs (umol)	[c] Mass AuNPs ($*10^{-6}$ g)	[d] Number AuNPs (ea/set)	[e] Volume AuNPs ($*10^{-7}$ nm^3/set)	[f] Mass AuNPs ($*10^{-13}$ g/set)	[g] Set ($*10^{6}$)	[h] Total number AuNPs ($*10^{10}$ ea)
0	0	0.2	15.8	1007	2.87	5.55	28.5	2.87
1	0.1036	0.0964	7.62	1063	3.56	6.87	11.1	1.18
2	0.1375	0.0625	4.94	1012	2.39	4.62	10.7	1.08
3	0.159	0.041	3.24	1152	5.47	10.6	3.07	0.353
4	0.155	0.045	3.55	1044	7.82	15.1	2.35	0.246
5	0.1498	0.0502	3.97	1025	9.66	18.7	2.13	0.218
6	0.1343	0.0657	5.19	1051	13.1	25.3	2.05	0.215
7	0.1363	0.0637	5.03	1120	20.9	40.3	1.25	0.140
30	0.1358	0.0642	5.07	106	37.3	72.9	0.70	0.00747

[a] The mass of $AuBr_2^-$ in the supernatant of the ripening solution after centrifugation (Figure S5)
[b] The approximate mass of the AuNPs determined by subtracting [a]the mass of $AuBr_2^-$ from the total mass of Au (0.2 μmol)
[c] Unit conversion of the approximate mass of AuNPs from moles to grams obtained by ICP-AES analysis.
[d] The number of AuNPs in over ten TEM images (Figure S1 (b))
[e] The total volume of AuNPs was estimated by considering their distinct size in PSD (Figure S1 (b)).
[f] The mass of AuNPs per set was obtained by dividing [e]the total volume of AuNPs per set by the density of Au.
[g] The approximate number of sets was obtained by dividing [c]the mass of the AuNPs by [f]the mass of AuNPs per set.
[h] The total number of AuNPs in the ripening system was approximated by multiplying [d]the number of AuNPs by [g]the approximate number of sets.